EMI in Modern AC Motor Drive Systems

Firuz Zare, Queensland University of Technology Brisbane, QLD, Australia Email: f.zare@qut.edu.au

Abstract—*In this paper, several aspects of high frequency related issues of modern AC motor drive systems, such as common mode voltage, shaft voltage and resultant bearing current and leakage currents, have been discussed. Conducted emission is a major problem in modern motor drives that produce undesirable effects on electronic devices. In modern power electronic systems, increasing power density and decreasing cost and size of system are market requirements. Switching losses, harmonics and EMI are the key factors which should be considered at the beginning stage of a design to optimise a drive system.*

Introduction

Nowadays, more than 60 percent of the world's energy is used to drive electric motors. Due to growing requirements of speed control, pulse width modulated inverters are used in adjustable speed drives. Rapid developments in semiconductor technology have increased the switching speed and frequency of power switches dramatically. In a motor drive system, a voltage source converter with hard switches generates high dv/dt, which causes leakage currents due to stray capacitances in an electric motor. As shown in Fig.1, a modern power electronic drive consists of a filter, a rectifier, a DC link capacitor, an inverter and an AC motor. Many small capacitive couplings exist in the motor drive systems which may be neglected at low frequency analysis but the conditions are completely different at high frequencies.

Electromagnetic Interference (EMI) is a major problem in recent motor drives that produces undesirable effects on electronic devices. In modern power electronic systems, increasing power density and decreasing cost and size of a system are market requirements. Switching losses, harmonics and EMI are the key factors which should be considered at the beginning stage of a design to optimise a drive system.

Common mode voltage creates shaft voltage through electrostatic couplings between a rotor and stator windings and the rotor and a frame which can cause bearing currents when the shaft voltage exceeds a breakdown voltage level of the bearing grease.

An increase in the carrier frequency of voltage-source Pulse Width Modulated (PWM) inverters based on high-speed switching devices has improved operating characteristics of the inverters. High speed switching can generate the following serious problems due to high dv/dt:

- Ground current escaping to earth through stray capacitors inside a motor
- Conducted and radiated noises
- Shaft voltage and bearing current

Models of parasitic couplings and high frequency components for an inverter fed induction motor drive system are investigated to determine suitable models to predict

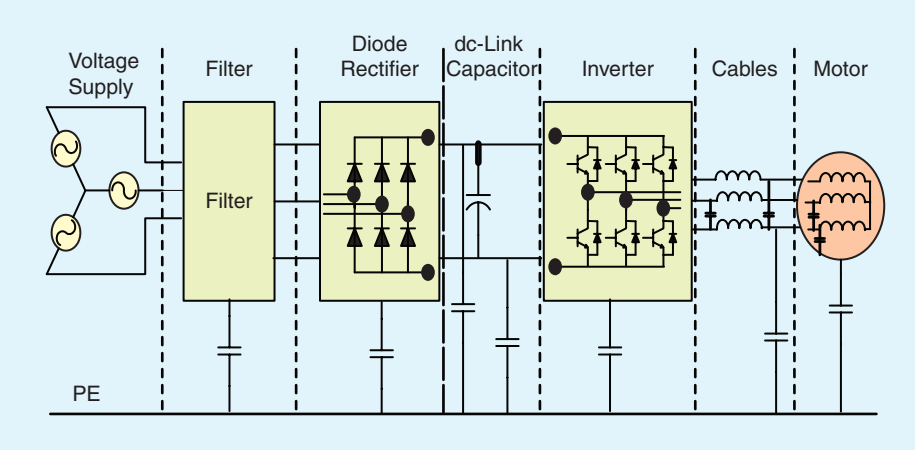

Fig. 1. A power electronic motor drive system with capacitive couplings.

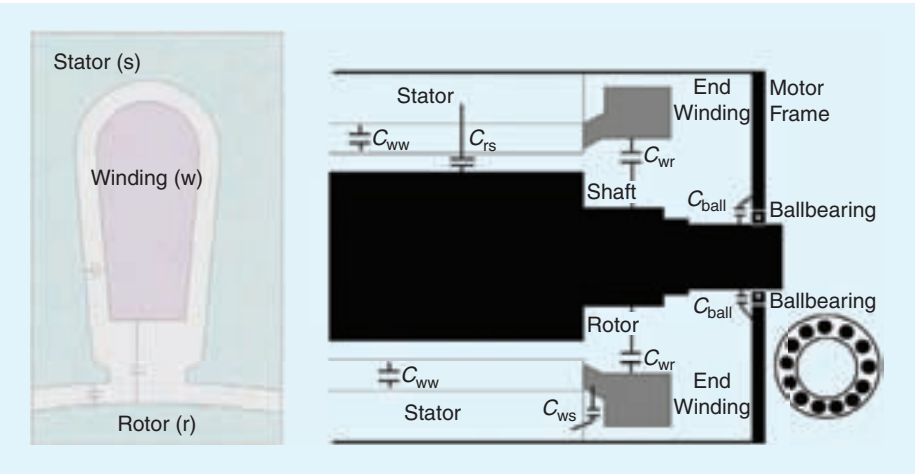

Fig. 2. A view of stator slot and capacitive coupling in an induction motor.

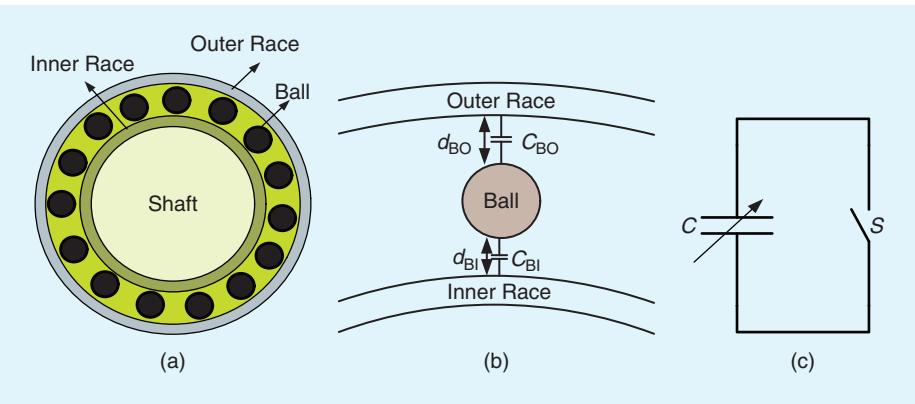

Fig. 3. (a) general structure of a ball bearing (b) a view of ball, outer and inner races and capacitive couplings (c) simple model of a ball bearing.

bearing currents and shaft voltage over a wide frequency range. A high frequency model of an electric motor is an important issue for power electronic engineers, which helps them to analyse leakage and bearing currents and to design EMI filters. At low frequency, an equivalent circuit of an electric motor consists of inductances and resistances without considering stray capacitances and skin effect. These issues become more important at high speed switching applications due to high dv/dt.

Fig.2 shows the capacitive couplings of an induction motor and a view of stator slot, where:

C_{wr} is the capacitive coupling between the stator winding and rotor

C_{ws} is the capacitive coupling between the stator winding and stator frame

C_{rs} is the capacitive coupling between the rotor and stator frame

C_{ww} is the capacitive coupling between turns of stator winding

C_{ball} is the capacitive coupling of ball bearing

Fig.3 shows a general structure of a ball bearing and shaft in an AC machine. As shown in this figure there are some balls between outer and inner races with lubricated grease between the balls and the races. There are capacitive couplings between the outer and inner races. During operation, the distances between the balls and races may be changed and will vary the capacitance values and resultant electric field between the races and balls. Due to this fact, this capacitance has a nonlinear value. Lubricated grease in the ball bearing cannot withstand a high voltage and a short circuit through the lubricated grease may happen, thus this phenomenon can be modelled as a switch.

PWM inverters have been found to be a major cause of motor bearing failures in inverter motor drive systems. All inverters generate common mode voltages relative to the ground, which make bearing current through motor parasitic capacitances.

According to Fig.4.a, phase voltages and a common mode voltage (V_n) can be derived based on the power converter voltages (V_a, V_b,V_c). Each leg voltage of a three phase inverter is given by:

$$\begin{aligned} V_a &= V_{an} + V_n \\ V_b &= V_{bn} + V_n \\ V_c &= V_{cn} + V_n \end{aligned} \qquad (1)$$

And then:

$$V_a + V_b + V_c = (V_{an} + V_{bn} + V_{cn}) + 3V_n \qquad (2)$$

It is clear that in a three-phase system:

$$V_{an} + V_{bn} + V_{cn} = 0 \qquad (3)$$

So, the common mode voltage can be calculated as:

$$V_n = (V_a + V_b + V_c)/3 \qquad (4)$$

In a three phase power inverter, a DC voltage is converted to three phase voltages with 120° phase shift. Fig.4.b shows three phase leg voltages of an inverter with common mode voltage.

The trend in increasing switching frequency improves the quality of current waveforms in motor drive systems but due to short switching time, a high dv/dt is produced across the motor terminal. The leakage current is created by a high voltage stress during switching time and capacitive coupling in an AC motor.

Fig.5 shows a simple equivalent model of an induction motor which contains main capacitances between the windings, rotor and the stator frame.

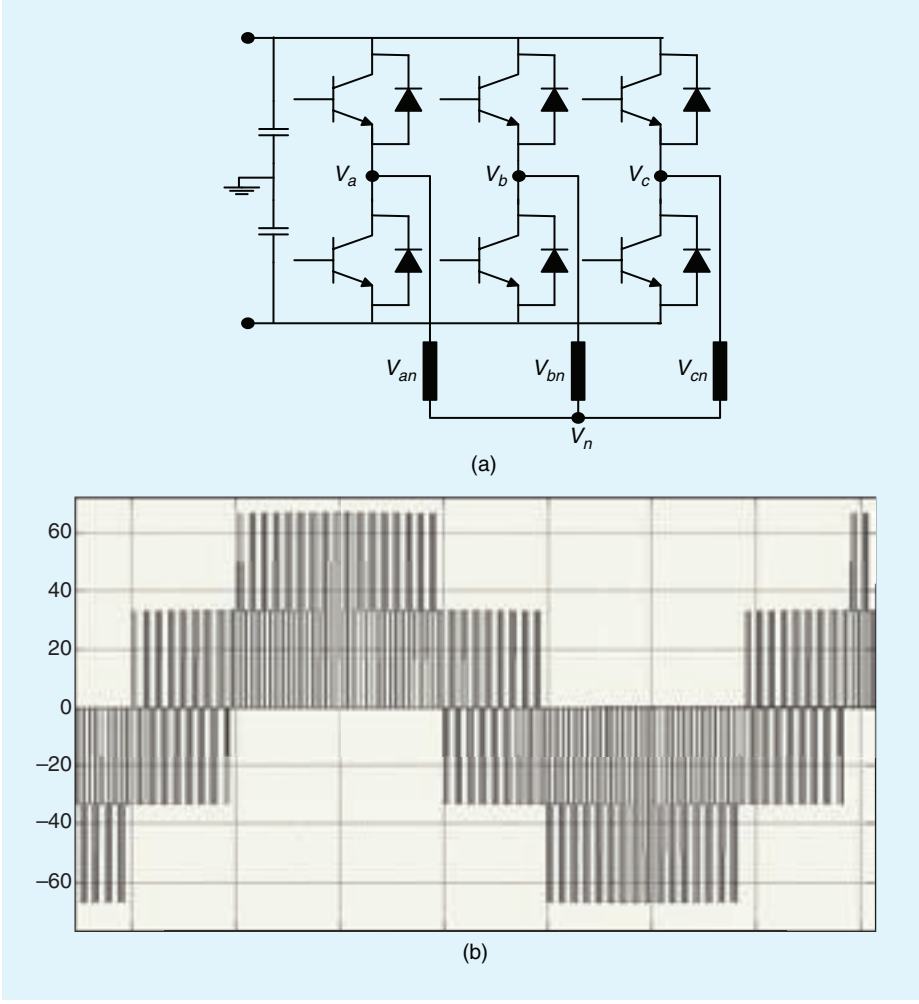

Fig. 4. (a) three phase voltage source inverter (b) PWM voltage.

Analysis of an Electric Motor at High Frequency

The stray capacitance between the windings and the stator frame is the most significant parasitic component compared to the other stray capacitances which generate significant conducted emission noise. At high frequency, an electric motor can be modeled as distributed capacitors, inductors and resistors as shown in Fig.6 and the maximum frequency can be determined using the standing wave's equation. We consider one ω section to model the motor at high frequency as shown in Fig.6.b and only the stray capacitance between the windings and the stator has been considered. Each motor has different high frequency parameters due to its structure, size and materials.

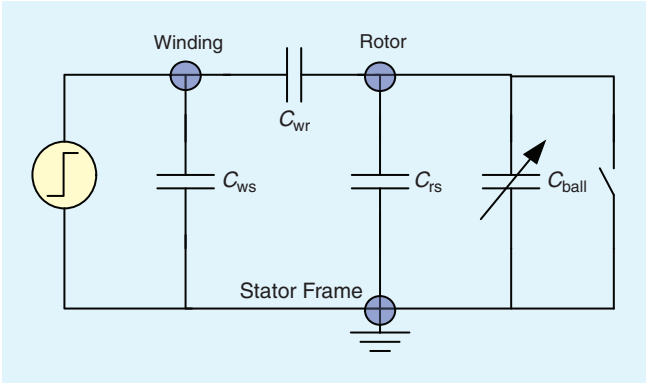

Fig. 5. A high frequency model of an induction motor.

Calculation of C_{ws}

The first step is to measure the magnitude and the phase values of the impedance in terms of frequency based on two different connections of the windings.

The first measurement is based on Fig.7.a where three phases are connected to each other at the terminal sides. Thus, the impedance between the phases and the stator (phase and magnitude values) can be measured in terms of the frequency using an impedance analyzer.

Based on this configuration, the impedance of the stray capacitance, C_{ws}, is much higher than the impedance of L_s and R_{loss} at low frequencies and the model can be simplified as two parallel stray capacitances.

Fig.8 shows measurement results of the impedance between the phases and the stator frame of a 5.5 KW motor. According to Fig.8, the phase value is around –90 at <40 KHz which addresses the fact that the two capacitors are connected to each other in parallel. The stray capacitance of the electric motor has been calculated using the magnitude and the phase values from 10 kHz up to 40 kHz and the result shows that C_{ws} is almost around 0.9 nF. The capacitance value is calculated based on the measurement results and $|Z_{c_{ws}}| = 1/\omega C_{ws}$.

Calculation of L_s and R_{loss}

The second measurement is based on Fig.7.b where three phases are connected to each other and the impedance between the phases and star point is measured. Based on this configuration, the impedance of the stray capacitance is much higher than the impedance of L_s and R_{loss} (Fig.9.a) at low frequencies

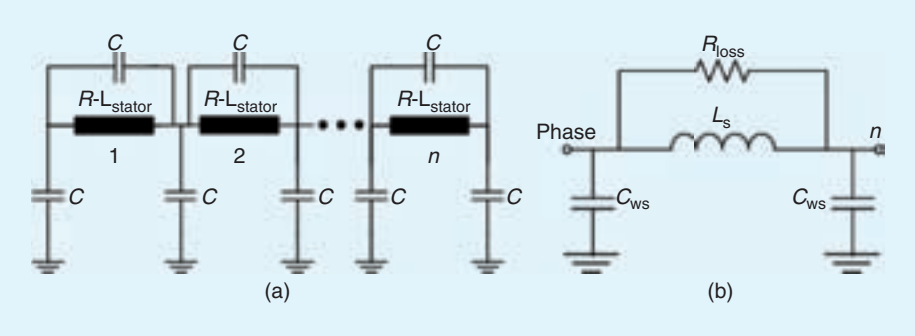

Fig. 6. (a) a distributed model of an electric motor at high frequency (b) a simple model of an electric motor.

and it can be simplified as an inductive and a resistive load as shown in Fig.9.b.

Fig.10 shows measurement results of the impedance between the phases and the star point. The inductance and resistance values can be calculated using the measurement results and based on the circuit diagram shown in Fig.9.b. The inductance value is decreased from 5.77 mH down to 5.56 mH when

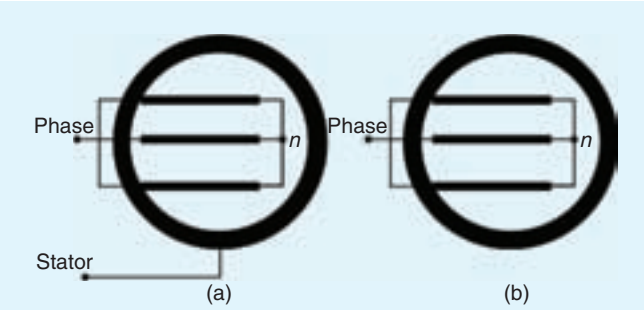

Fig. 7. Two different connections to measure the impedance between (a) the phases and the stator (b) the phases and the star point.

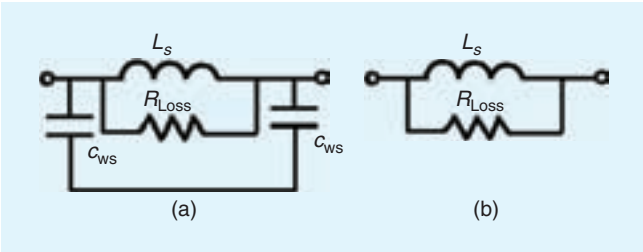

Fig. 9. Circuit diagram for measurement between phases and star point (a) a model of motor (b) simplified model for low frequency range.

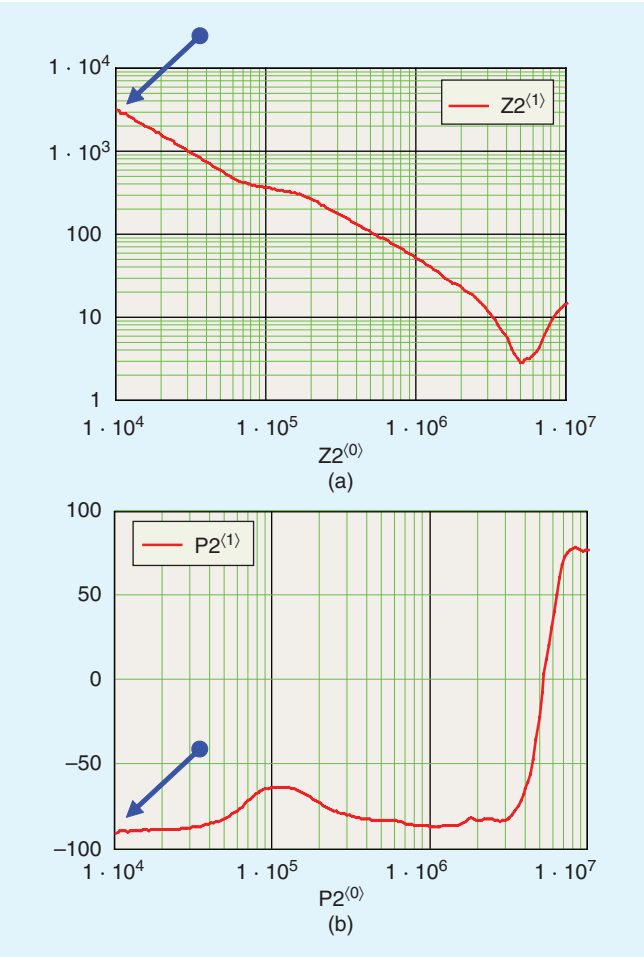

Fig. 8. Measurement results (a) magnitude and (b) phase values between the phases and the stator of a 5.5 KW motor.

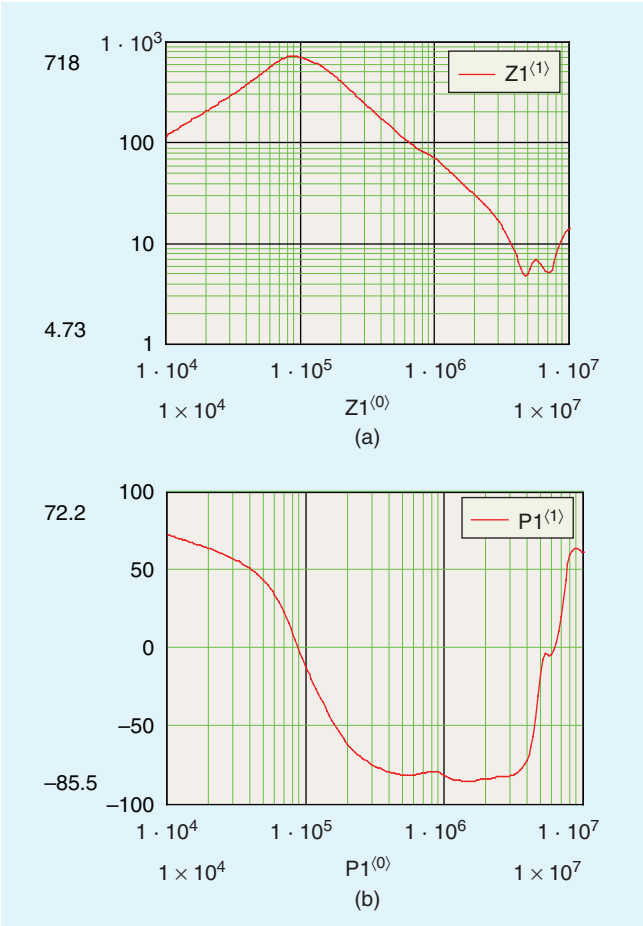

Fig. 10. Measurement results (a) magnitude and (b) phase values between the phases-star point of a 5.5 KW motor.

the frequency is increased from 10 kHz up to 40 kHz. At low frequency (below 100 kHz), the input impedance of the windings (according to Fig.9.b) is $Z_{RL} = R_{loss} \times j\omega L_s / j\omega L_s + R_{loss}$. The magnitude and phase values of this configuration, which are used to extract the resistance and inductance values, are given in Fig.10.

The simulations have been carried out based on the following equations driven from the above figures:

$$Z_{stator\_winding} = \frac{Z_{C_{ws}}(Z_{RL} + Z_{C_{ws}})}{2 \times Z_{C_{ws}} + Z_{RL}}$$

$$Z_{winding\_winding} = \frac{\frac{Z_{C_{ws}}}{2}(Z_{RL})}{\frac{Z_{C_{ws}}}{2} + Z_{RL}}$$

Where $Z_{RL} = R_{loss} \times j\omega L_s / j\omega L_s + R_{loss}$ and $|Z_{c_{ws}}| = 1/\omega C_{ws}$

There is a short cable from the motor terminals to the impedance analyzer, which can be modeled as a R_L in series with the motor as shown in Fig.11. The second resonance frequency shown in Fig.10 is associated with this inductance and the first stray capacitance, C_{ws}. Thus the inductance value of the cable can be calculated using $L_{cable} = 1/(2\pi f)^2 C_{ws} = 378$ nH. The resistance value of the cable can be calculated at the second resonance frequency. Based on this analysis, the parameters of the 5.5 kW motor have been extracted as follow:

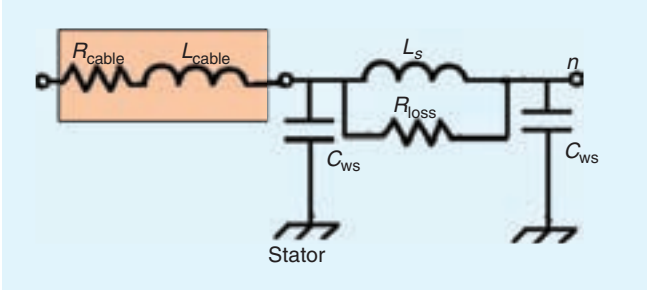

Fig. 11. A high frequency model of a motor with a short cable.

$L_s = 5.56$mH; $C_{ws} = 0.9$nF; $R_{loss} = 2215\,\Omega$; $L_{cable} = 378$nH; $R_{cable} = 3\,\Omega$

The 5.5 kW motor is modeled based on this analysis and the simulation and experimental results are shown in Fig.12. The cable impedance is negligible at frequencies below 4-5 MHz but it becomes significant above that frequency range.

Active EMI Filters

The use of Active EMI filters based on current injection is a proper solution to cancel common mode high frequency currents. Fig.13 shows a block diagram of an active EMI filter with a common mode transducer.

The filter composes of an emitter follower using complementary transistors and a common mode transformer to measure the

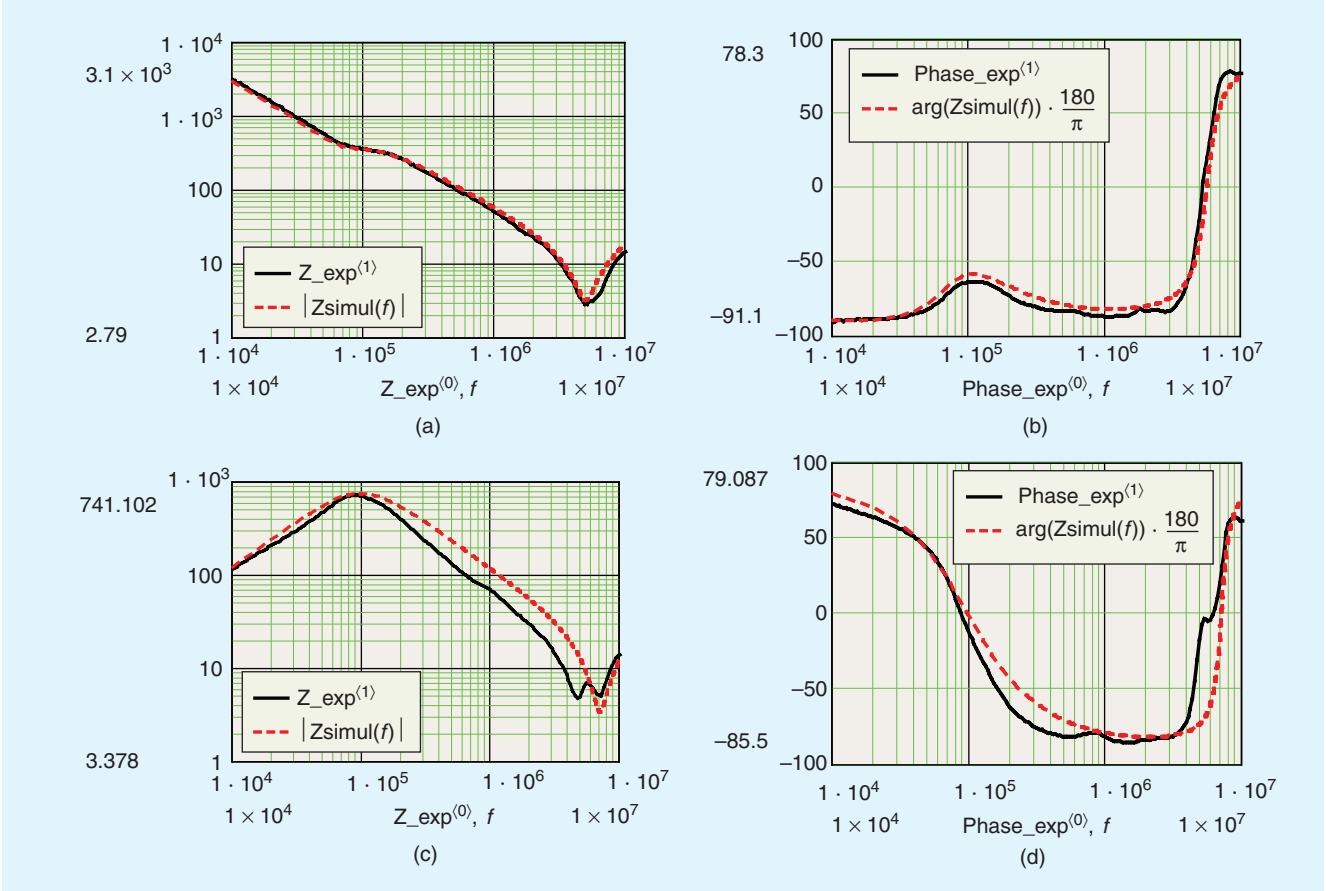

Fig. 12. Experimental and simulation results of a 5.5 kW motor; (a) magnitude (b) phase values between phases-stator (c) magnitude (d) phase values between phases-star point.

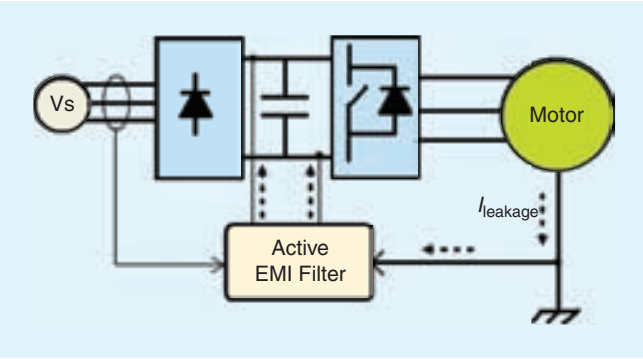

Fig. 13. An active EMI filter.

leakage current. A high frequency amplifier generates the same current and injects it into the motor drive circuit in order to bypass the current as shown in Fig.13. In this case, the leakage current generated by dv/dt is circulated through the active filter.

There are few issues to design an active EMI filter which should be considered:

- A high band width power amplifier to generate the leakage current
- A three-phase or a single-phase current transducer with symmetrical configuration to measure current accurately
- A separate power supply for the active EMI filter.

Conclusions

A high frequency model of an electric motor has been analyzed in this paper. One of the advantages of the high frequency model of the electric motor is to estimate and analyze the leakage and bearing currents to design EMI filters using simulations. This paper addresses a simple method to extract high frequency parameters of an electric motor based on the measurement results. It is recommended to estimate the behavior of the motor in a frequency range, when the motor acts as a capacitive or an inductive load according to the phase values of the impedance. Then, the parameters can be calculated directly from the magnitude and the phase values of the impedance.

In this paper several aspects of high frequency related issues of modern AC motor drive systems, such as common mode voltage, shaft voltage and resultant bearing current and leakage currents, have been discussed. Conducted and radiated emissions are major problems in modern motor drives that produce undesirable effects on electronic devices. In modern power electronic systems, increasing power density and decreasing cost and size of system are market requirements. Switching losses, harmonics and EMI are the key factors which should be considered at the beginning stage of a design to optimise a drive system. In most power electronic designs, EMI issues have not been taken into account as one of the main factors; and mitigation techniques for EMI are considered at the last stage of design!

References

[1] Firuz Zare, "Power Electronics E-Book", www.peeeb.com; from this website, you can virtually attend lectures and tutorials and also access to lecture notes and computer Labs.

[2] Firuz Zare, "High frequency model of an electric motor based on measurement results", Australian Journal of Electrical & Electronics Engineering (AJEEE), Vol 4, No 1, 2008, page 17-24.

Biography

Dr. Firuz Zare *received his B.Eng degree in Electronic Engineering from Gilan University, his MSc degree in Power Engineering from K.N Toosi University and his Ph.D. degree in Power Electronics from Queensland University of Technology in 1989, 1995 and 2001, respectively. He spent several years in industry as a team leader and development engineer where he was involved in electronics and power electronics projects. Dr. Zare won a student paper prize at the Australian Universities Power Engineering Conference (AUPEC) conference in 2001 and was awarded a Symposium Fellowship by the Australian Academy of Technological Science and Engineering in 2001. He received the Vice Chancellor's Award in research in 2009 and faculty excellence award in research as an early career academic from Queensland University of Technology in 2007. Dr. Zare has published over 60 journal and conference papers and technical reports in the area of Power Electronics. He has been invited as a reviewer and technical chair of national and international conferences and presented several seminars and workshops. He presented a half-day tutorial at the 2007 IEEE International Symposium on EMC in Hawaii, at the EMC Asia Pacific Workshop in Singapore in May 2008 and at the 2008 IEEE International Symposium on EMC in Michigan. Dr. Zare is a senior lecturer at the Queensland University of Technology, Australia and a senior member of the IEEE.* **EMC**